Stochastic Acceleration in Turbulent Electric Fields Generated by 3D Reconnection

Marco Onofri, Heinz Isliker, and Loukas Vlahos
Department of Physics, University of Thessaloniki, 54124 Thessaloniki, Greece
(Received 9 February 2006; published 19 April 2006)

Electron and proton acceleration in three-dimensional electric and magnetic fields is studied through test particle simulations. The fields are obtained by a three-dimensional magnetohydrodynamic simulation of magnetic reconnection in slab geometry. The nonlinear evolution of the system is characterized by the growth of many unstable modes and the initial current sheet is fragmented with formation of small scale structures. We inject at random points inside the evolving current sheet a Maxwellian distribution of particles. In a relatively short time (less than a millisecond) the particles develop a power-law tail. The acceleration is extremely efficient and the electrons absorb a large percentage of the available energy in a small fraction of the characteristic time of the MHD simulation, suggesting that resistive MHD codes are unable to represent the full extent of particle acceleration.

DOI: 10.1103/PhysRevLett.96.151102 PACS numbers: 96.60.qe, 52.35.Vd, 52.65.Cc, 96.60.Iv

It is widely accepted that magnetic reconnection plays a significant role in converting magnetic energy to thermal energy and kinetic energy of electrons and protons in laboratory plasmas, the Earth's magnetosphere, the solar corona, and in extragalactic jets [1,2].

In resistive magnetohydrodynamic models, resistivity breaks the frozen-in law in a boundary layer, allowing reconnection to occur. A current sheet can be spontaneously unstable to resistive instabilities, like the tearing modes, which lead to magnetic reconnection [3]. Many numerical codes have been developed to study the nonlinear evolution of tearing modes in two-dimensional approximations [4]. However, three-dimensional effects may become important in modifying the spatial structure of the current sheets and the reconnection rate [5].

Different numerical studies have been performed to investigate collisionless magnetic reconnection using fluid models, where magnetic reconnection is made possible by electron inertia, and kinetic simulations, in two- and three-dimensional configurations [6,7]. It has been shown that in the three-dimensional kinetic reconnection the characteristic time scale of the instability is much faster than that of the two-dimensional tearing mode instability.

The change of the topology of the magnetic field due to magnetic reconnection allows the release of magnetic energy, which can be responsible for the acceleration of particles. In two-dimensional reconnection configurations particle acceleration has been extensively studied both analytically and numerically [8]. The acceleration is caused by the motion of particles along the electric field in the current sheet, but the magnetic field plays a significant role since it influences the trajectory and therefore the energy gain of the particles. Recently, it has become clear that it is essential to include in the model the longitudinal component of the magnetic field, which is parallel to the electric field in the current sheet [9]. Studies of particle acceleration with a longitudinal magnetic field component have also been performed for the case of a magnetic x line [10]. Moreover, particle acceleration has been studied through numerical simulations in the framework of two-dimensional resistive and collisionless reconnection [11,12].

All these studies have been performed for simple electric and magnetic field configurations, with homogeneous electric fields, the investigation of more complex three-dimensional configurations has though shown that more realistic simulations are necessary to understand particle acceleration in reconnection regions [13]. Test particle simulations in three-dimensional electric and magnetic fields, obtained by magnetohydrodynamic simulations of magnetic reconnection, have shown that idealized analytical two-dimensional treatments are too simplified models, which cannot give a complete understanding of the problem [14].

In the present Letter, we focus our attention on a single current sheet and its fragmentation, as yielded by a resistive magnetohydrodynamics simulation of three-dimensional magnetic reconnection. The initial equilibrium magnetic field includes a longitudinal component, parallel to the current sheet, as this was recognized to be an important characteristic to understand the acceleration of particles. We study the acceleration of electrons and ions in the electromagnetic fields that result from the evolution of this current sheet and discuss the limitations of the MHD approach to reconnecting plasmas and the importance of kinetic effects.

We numerically solve the incompressible, dissipative, magnetohydrodynamics (MHD) equations in dimensionless units in a three-dimensional Cartesian domain, with kinetic and magnetic Reynolds numbers $R_v = 5000$ and $R_M = 5000$. We set up the initial condition in such a way to have a plasma that is at rest, in the frame of reference of our computational domain, permeated by an equilibrium magnetic field $\mathbf{B}_0$, sheared along the $\hat{x}$ direction, with a current sheet in the middle of the simulation domain

$$\mathbf{B}_0 = B_{y0}\hat{y} + B_{z0}(x)\hat{z}, \quad (1)$$

where B_{y0} is a constant value, which has been set to 0.5 and

B_{z0} is given by

$$B_{z0}(x) = \tanh\left(\frac{x}{0.1}\right) - \frac{x/0.1}{\cosh^2(\frac{1}{0.1})}. \quad (2)$$

In the y and z directions, the equilibrium magnetic field is uniform and we impose periodic boundary conditions, since we do not expect any important boundary effects on the development of turbulence. In the inhomogeneous x direction, we impose fixed boundary conditions. We perturb these equilibrium fields with three-dimensional divergenceless fluctuations.

The nonlinear evolution of the system is characterized by the formation of small scale structures, especially on the lateral regions of the computational domain, and coalescence of magnetic islands in the center. This behavior is reflected in the three-dimensional structure of the electric field, which shows that the initial equilibrium is destroyed by the formation of current filaments. For details about this MHD simulation see [5]. After about $t = 50\tau_A$ (where τ_A is the Alfvén time) the current sheet starts to be fragmented, as can be seen in Fig. 1, where we show the configuration of the electric field $\mathbf{E} = \eta\mathbf{J} - \mathbf{v} \times \mathbf{B}$ calculated from the MHD simulation. Figure 1 shows the isosurfaces of the electric field at different times calculated for two different values of the electric field: the red surface represents higher values and the blue surface represents lower values. The structure of the electric field is characterized by small regions of space where the field is stronger, surrounded by a larger volume occupied by lower electric field values. At later times the fragmentation is more evident, and at $t = 400\tau_A$, the initial current sheet has been completely destroyed and the electric field is highly fragmented. The strong electric field regions are acceleration sites for the particles and their distribution in space fills a larger portion of the simulation box at later times, with increasing possibility to accelerate a higher number of particles.

To give a measure of the fragmentation of the electric field, we calculated the fractal dimensions of the fields shown in Fig. 1, using the box counting definition of the fractal dimension. The thresholds are the same that have been used to draw the isosurfaces shown in Fig. 1. For the fields represented by the blue surfaces in Fig. 1, we found fractal dimensions $d = 2$, $d = 2.5$, and $d = 2.7$ at $t = 50\tau_A$, $t = 200\tau_A$, and $t = 400\tau_A$, respectively. For the more intense electric fields (red surfaces in Fig. 1), the fractal dimensions are $d = 1.8$, $d = 2$, and $d = 2.4$ at $t = 50\tau_A$, $t = 200\tau_A$, and $t = 400\tau_A$, respectively. These fractal dimensions can be considered as a way to quantify the degree of fragmentation of the electric field and the fraction of space it fills as it evolves in time.

We calculate the magnitude E of the electric field at each gridpoint of the simulation domain and construct the distribution function of these quantities, which is shown in Fig. 2 for $t = 50\tau_A$. We separately plot the resistive and the convective component of the electric field. The resistive part is less intense than the convective part, but it is much more important in accelerating particles, as we verified by performing some simulations where only one of the two components was used. In the simulations described in this article both components of the electric field have been included.

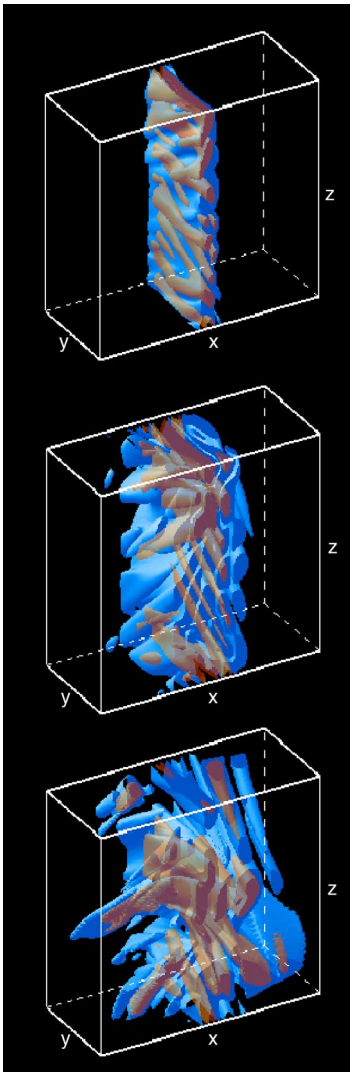

FIG. 1 (color online). Electric field isosurfaces at $t = 50\tau_A$, $t = 200\tau_A$, and $t = 400\tau_A$.

Protons and electrons are injected into the simulation box where they move under the action of the electric and magnetic fields, which do not evolve during the particle motion. This is justified by the fact that the evolution of the fields is much slower than the acceleration process, electrons and ions are accelerated on a short time scale to very high energies, and in such short times the fields would not change significantly according to the MHD simulation.

The trajectories of the test particles inside the box are calculated by solving the relativistic equations of motions, using a fourth order Runge Kutta adaptive step-size scheme. Since the magnetic and the electric fields are given only at a discrete set of points (the grid-points of the MHD

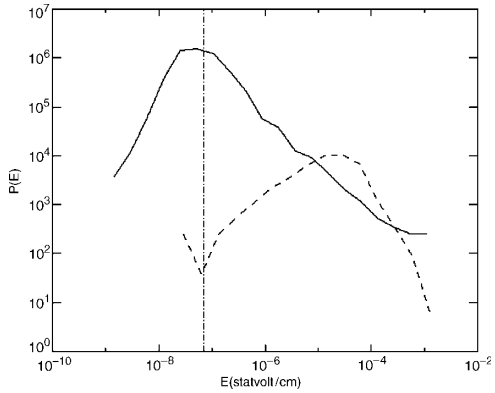

FIG. 2. Distribution function of the resistive (solid line) and convective (dashed line) electric field at $t = 50\tau_A$. The vertical line represents the value of the Dreicer field in the solar corona.

simulation), both fields are interpolated with local three-dimensional linear interpolation to provide the field values in between grid points.

The configuration studied here can be applied to many astrophysical situations where magnetic reconnection is produced by the development of resistive instabilities in a current sheet. Particularly detailed information on the accelerated particles is contained in the recent data from the Ramaty High Energy Solar Spectroscopic Imager (RHESSI) satellite obtained from solar flares [15], which allow a detailed comparison with models for particle acceleration. We thus have chosen physical values in the simulations that are relevant for the solar corona: $B_0 = 100G$, $n_0 = 10^9$ cm^{-3}, and $l_x = 10^9$ cm. The corresponding value of the resistivity is $\eta \simeq 2 \times 10^{-6}$ s. The Dreicer field, which is represented by the vertical line in Fig. 2, is $E_D \simeq 7 \times 10^{-8}$ statvolt/cm. In each case 50 000 test particles (protons or electrons) are injected in the simulation box with random initial positions and the three components of the particle initial velocities are randomly drawn from a Gaussian distribution with a temperature of 1.16×10^6 K. The electric and magnetic fields used to accelerate the particles are obtained from the MHD simulation at $t = 50\tau_A$, which corresponds to $t \simeq 72$ s. Most of the resistive and all of the convective electric fields are super-Dreicer. The total available magnetic energy inside the simulation volume is $W_B = \int (B_0^2/8\pi) dV \sim 10^{32}$ erg. The particles are followed for a time t_p, much shorter than the time scale on which the magnetic configuration evolves. The energy distribution is calculated from the kinetic energy at the time t_p for the particles that are still in the simulation box and from the energy at the time they exit the simulation box for the particles that escaped.

For the case of electrons, the particles' energy distribution at different times is shown in Fig. 3. Some of the test particles are quickly accelerated to high energies so that the initial Maxwellian distribution changes, developing a tail that grows in time. The kinetic energy of the electrons increases very rapidly, and in a short time it equals the energy contained in the magnetic field. Since there is no backreaction of the particles onto the fields, there is no limit to the energy they can gain until they leave the simulation box. For this reason we follow the particle motion only as long as their energy is still less than 50% of the magnetic field energy W_B, which is up to $t_{\rm pe} = 8 \times 10^{-5}$ s. The maximum kinetic energy at the end of the run turns then out to be about 1 MeV. Collisions are not included in the simulations because the collisional time is about $t_c = 5.5 \times 10^{-3}$ s, which is much longer than $t_{\rm pe}$. In the final distribution, the logarithmic slope of the power-law tail is $\simeq 1$. The power-law tails of the distributions start at an energy of about 1 keV. The total number of particles contained in the tail of the distributions ($E_K \geq 1$ keV) is $\simeq 6 \times 10^{37}$ for the assumed values of the particle density n_0 and length l_x. Below 1 keV, the electrons have a thermal distribution. As we explained in the introduction, it was found in previous works that substantial acceleration of particles also occurs in a two-dimensional current sheet. Therefore, results similar to those reported here for $t = 50\tau_A$, where the fragmentation of the current sheet has developed, start to appear at earlier times, but with fewer particles in the tail of the distribution.

Turning to protons, we find that acceleration is much less efficient than for electrons, only at $t_{\rm pi} = 3 \times 10^{-3}$ s they reach a maximum kinetic energy of about 1 MeV, with energy distributions that are similar to those of the electrons. Because of the much slower acceleration time scale of the protons, the time limit for our simulation is determined by the electrons, $t_{\rm pe}$ ($t_{\rm pe} \ll t_{\rm pi}$)—at times as large as $t_{\rm pi}$, the electrons would have absorbed all the available magnetic energy W_B. At the time limit $t_{\rm pe}$ then, the distribution of the ions has remained close to the initial Maxwellian, with just minor gain in energy.

Since solar flares are closely associated with magnetic reconnection, the data obtained by the RHESSI satellite can be used to validate theoretical ideas related to the acceleration of particles during magnetic reconnection [2]. The main constraints reported from the current RHESSI

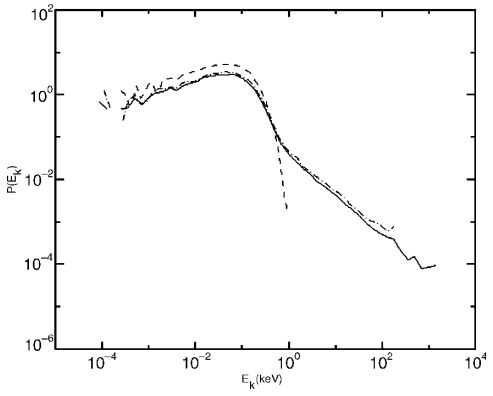

FIG. 3. Distribution function of electron kinetic energy at $t = 8 \times 10^{-5}$ s (solid line), $t = 3 \times 10^{-5}$ s (dot-dashed line), and the initial distribution (dashed line). The electromagnetic field is given at $t = 72$ s.

data are (1) the energy distribution, inferred from the analysis of the hard x rays, is thermal up to an energy of 10–15 KeV and is smoothly continued to a power-law distribution with index around 1 to 5 at higher energies; (2) the accelerated electrons can reach a maximum energy of 1 MeV, and the ions a maximum energy of several hundreds of MeV; (3) the high energy particles absorb more than 50% of the energy released in a solar flare [15,16].

The results of our simulations show that a decayed and fragmented current sheet can be a very efficient accelerator. The particles absorb a large amount of energy from the magnetic field in a short time, and the magnetic and electric fields lose a large fraction of their energy. The backreaction of the particles is though not taken into account in the test particle simulations reported here, which in this sense are not self-consistent. Our results suggest that the lifetime of a current sheet of this size in the solar corona is very short since energetic particles absorb a large fraction of the available magnetic energy. As a consequence of the backreaction, the magnetic and electric field would change more quickly than what the MHD simulation shows, the acceleration process can be expected to be slower, and the resulting energy distributions could probably be different.

The limitations of the presented approach, in the case of the electrons, are reflected in the problems of our results to reproduce all the characteristics of the distributions that are observed in solar flares (e.g., variation of power-law slopes). In the case of the ions, the situation is different. Their maximum energy at the time limit of our simulations is lower than the energy that protons usually reach during solar flares. We can thus conclude that ions are not accelerated to the high energies observed during solar flares by single, isolated, turbulent current sheets. Stressed and complex large scale magnetic topologies can though form simultaneously many current sheets [17], and it has been shown that the interaction of the ions (and electrons) with many current sheets can be a very efficient accelerator [18,19].

Ideal and resistive MHD codes, used widely in many astrophysical applications, reach the limits of their applicability as soon as current sheets start to form. Then the acceleration of electrons will start to dominate the evolution of the current sheet, and kinetic phenomena become important.

The fast acceleration that we observe in the simulation is also due to the high (anomalous) resistivity that we use and the consequent high values of the parallel electric field. Such a value of the resistivity is necessary, from a practical point of view, in order to simulate the process of reconnection in reasonable CPU time, and, in astrophysical terms, to release the observed magnetic energy on a time scale comparable to the flare process. Anomalous resistivity is realistic only in limited regions (where thin current sheets are formed) in the solar corona. Classical resistivity, which is extremely small in the corona, is appropriate for the slow evolution of the large scale magnetic structures prior to the formation of the current sheets.

In summary, if large scale 3D current sheets are formed in the solar corona, they evolve slowly in the beginning and soon collapse, forming a turbulent super-Dreicer electric field environment. These fragmented current sheets are very efficient electron accelerators and mark the end of the applicability of MHD. MHD is not a good approximation to describe the entire process of reconnection in the range of parameters that is of interest for fast magnetic dissipation and particle acceleration, and a self-consistent kinetic treatment becomes necessary.

This work was supported by the Research Training Network, funded by the European Commission (Contract No. HPRN-eT-2001-00310).

[1] D. Biskamp, *Magnetic Reconnection in Plasmas* (Cambridge University Press, Cambridge, England, 2000).
[2] E. R. Priest and T. Forbes, *Magnetic Reconnection: MHD Theory and Applications* (Cambridge University Press, Cambridge, England, 2000).
[3] H. P. Furth, J. Killen, and M. N. Rosenbluth, Phys. Fluids **6**, 459 (1963).
[4] F. Malara, P. Veltri, and V. Carbone, Phys. Fluids B **4**, 3070 (1992).
[5] M. Onofri, L. Primavera, F. Malara, and P. Veltri, Phys. Plasmas **11**, 4837 (2004).
[6] D. Borgogno, D. Grasso, F. Porcelli, F. Califano, F. Pegoraro, and D. Farina, Phys. Plasmas **12**, 032309 (2005).
[7] J. Buchner, Astrophys. Space Sci. **264**, 25 (1998).
[8] S. W. H. Cowley, Planet. Space Sci. **26**, 539 (1978).
[9] Y. E. Livitenko and B. V. Somov, Sol. Phys. **146**, 127 (1993).
[10] R. L. Kaufman, C. Lu, and D. J. Larson, J. Geophys. Res. **99A**, 11 277 (1994).
[11] B. Kliem, Astrophys. J. Suppl. Ser. **90**, 719 (1994).
[12] J. F. Drake, M. A. Shay, and W. Thongthai, Phys. Rev. Lett. **94**, 095001 (2005).
[13] J. Birn, M. F. Thomsen, J. E. Borovsky, G. D. Reeves, D. J. McComas, and R. D. Belian, J. Geophys. Res. **103**, 9235 (1998).
[14] R. Shopper, G. T. Birk, and H. Lesh, Phys. Plasmas **6**, 4318 (1999).
[15] R. P. Lin, Astrophys. J. **595**, L69 (2003).
[16] E. P. Kontar, A. G. Emslie, M. Piana, A. M. Massone, and J. C. Brown, Sol. Phys. **226**, 317 (2005).
[17] K. Galsgaard and A. Nordlund, J. Geophys. Res. **101**, 13 445 (1996).
[18] R. Turkmani, L. Vlahos, K. Galsgaard, P. J. Cargill, and H. Isliker, Astrophys. J. **620**, L59 (2005).
[19] L. Vlahos, H. Isliker, and F. Lepreti, Astrophys. J. **608**, 540 (2004).